CHEMISTRY
A EUROPEAN JOURNAL

DOI: 10.1002/chem.200601325

Ionic Hydrogen Bonds Controlling Two-Dimensional Supramolecular Systems at a Metal Surface

Dietmar Payer,[a] Alessio Comisso,[b] Alexandre Dmitriev,[a] Thomas Strunskus,[c] Nian Lin,*[a] Christof Wöll,[c] Alessandro DeVita,[b, d] Johannes V. Barth,[e, f] and Klaus Kern[a, f]

Abstract: Hydrogen-bond formation between ionic adsorbates on an Ag(111) surface under ultrahigh vacuum was studied by scanning tunneling microscopy/spectroscopy (STM/STS), X-ray photoelectron spectroscopy (XPS), near-edge X-ray absorption fine structure (NEXAFS), and molecular dynamics calculations. The adsorbate, 1,3,5-benzenetricarboxylic acid (trimesic acid, TMA), self-assembles at low temperatures (250–300 K) into the known open honeycomb motif through neutral hydrogen bonds formed between carboxyl groups, whereas annealing at 420 K leads to a densely packed quartet structure consisting of flat-lying molecules with one deprotonated carboxyl group per molecule. The resulting charged carboxylate groups form intermolecular ionic hydrogen bonds with enhanced strength compared to the neutral hydrogen bonds; this represents an alternative supramolecular bonding motif in 2D supramolecular organization.

Keywords: ab initio calculations · carboxylic acids · hydrogen bonds · scanning tunneling microscopy · supramolecular self-assembly

Introduction

Supramolecular self-assembly of molecular building blocks on well-defined substrates provides appealing opportunities to engineer low-dimensional nanostructures.[1] Molecules with functional groups for hydrogen bonding have been widely employed, especially carboxyl groups because of their ability to form self-complementary dimer synthons, that is, pairing of OH···O hydrogen bonds, which enhances the strength of the hydrogen bonding considerably.[2,3] A crucial requirement in the stability of these structures is the integrity of the carboxyl groups upon adsorption onto surfaces, as it was shown that under certain conditions the carboxyl groups may undergo deprotonation to create carboxylate functions.[4–11] This process destabilizes the dimer synthons and introduces new possibilities for intermolecular interactions. In particular, if the carboxylate groups stay charged upon adsorption onto a surface, this could enable the formation of stronger intermolecular ionic hydrogen bonds, which are a special class of hydrogen bonds that form between ionic donors (acceptors) and neutral acceptors (donors) and have bond strength up to one-third of the strength of covalent bonds.[12,13] Ionic hydrogen bonds may represent a new type of motif-controlling functional elements to assemble supramolecular structures at surfaces under solvent-free conditions. To understand the role of ionic hydrogen bonds in supramolecular assembly processes we studied 1,3,5-benzenetricarboxylic acid (trimesic acid, TMA) (Figure 1, inset) on Ag(111) under ultrahigh vacuum as a model system by scanning tunneling microscopy (STM),

[a] D. Payer, Dr. A. Dmitriev, Dr. N. Lin, Prof. Dr. K. Kern
Max Planck Institut für Festkörperforschung
Heisenbergstraße 1, 70563 Stuttgart (Germany)
Fax: (+49) 711-689-1662
E-mail: n.lin@fkf.mpg.de

[b] A. Comisso, Prof. Dr. A. DeVita
INFM-DEMOCRITOS National Simulation Center and
Center of Excellence for Nanostructured Materials (CENMAT)
University of Trieste (Italy)

[c] Dr. T. Strunskus, Prof. Dr. C. Wöll
Lehrstuhl für Physikalische Chemie 1
Ruhr Universität Bochum, Universitätsstraße 150
44780 Bochum (Germany)

[d] Prof. Dr. A. DeVita
Physics Department
King's College London
Strand, London WC2R 2LS (UK)

[e] Prof. Dr. J. V. Barth
Departments of Chemistry and Physics & Astronomy
University of British Columbia, Vancouver, B.C. V6T 1Z4 (Canada)

[f] Prof. Dr. J. V. Barth, Prof. Dr. K. Kern
Institut de Physique des Nanostructures
Ecole Polytechnique Fédérale de Lausanne, 1015 Lausanne (Switzerland)

scanning tunneling spectroscopy (STS), X-ray photoelectron spectroscopy (XPS), near-edge X-ray absorption fine structure (NEXAFS), and molecular dynamics calculations. Our previous study showed that TMA forms a honeycomb network structure mediated by neutral hydrogen bonds at room temperature.[5] Here we show that upon annealing above 300 K the carboxyl groups of the TMA molecules are gradually deprotonated. Above 420 K one out of three carboxyl groups per TMA molecule is deprotonated, and an irreversible phase transformation occurs. The new phase is densely packed, stabilized by ionic hydrogen bonds between the remaining carboxyl groups and the charged carboxylate moieties. The ionic hydrogen bonds effectively overcome the Coulomb repulsion between the charged species. To our knowledge this is the first time that ionic hydrogen bonds and their role in supramolecular organization under solvent-free, "dry", ultrahigh-vacuum conditions have been comprehensively studied. Our findings deepen the understanding of hydrogen bonding in the vicinity of metal surfaces and expand the design capabilities to realize 2D supramolecular systems.

Results and Discussion

Experimental results: Figure 1a shows an STM topograph of the TMA structure after annealing the sample to 300 K. The molecules are aggregated into the known honeycomb structure in which each molecule is connected to three neighboring molecules through carboxylic acid dimer synthons between the carboxyl groups. This gives a hexagonal lattice with a lattice constant of 1.78 ± 0.05 nm and an O···O distance in the hydrogen bonds of 0.34 ± 0.05 nm, in agreement with previous results obtained with TMA on other substrates.[11,14–16] Attempts to determine the registry of the honeycomb structure with respect to the Ag(111) surface were not successful, because we could not resolve the Ag(111) atomic lattice and the honeycomb structure simultaneously.

The ST spectra acquired on the clean Ag(111) surface show a sharp steplike feature with an onset at an energy E_0 of -70.9 ± 5.3 mV and a width of 10.6 ± 8.4 mV. In contrast

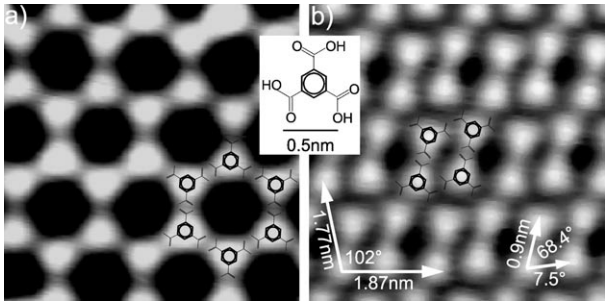

Figure 1. STM topographs of a) the honeycomb and b) quartet structures formed at 300 and 420 K, respectively. In both topographs the triangular appearance of the TMA molecules indicates flat-lying molecules. The inset shows the molecular model of the TMA molecules. Tentative models are superimposed on the STM data. Tunneling current: 0.5 nA, bias voltage: 0.5 V.

ST spectra acquired on the honeycomb phase show an onset at -9.7 ± 9.8 mV and are broadened to 17.1 ± 20.5 mV with the flat plateau extending above 1500 mV, as shown in Figure 2. Because there is no significant difference between

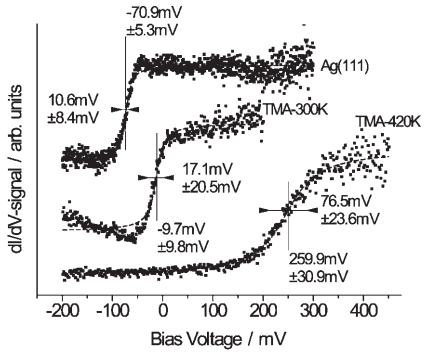

Figure 2. ST spectra acquired on clean Ag(111), the honeycomb structure, and the quartet structure. The spectra were normalized to a constant onset height and shifted along the *y* axis for better discrimination.

ST spectra taken at different positions of the TMA honeycomb structure, we can rule out that the onset is a signature of TMA molecular orbitals. We attribute this onset to the surface state formed by a two-dimensional electron gas, but shifted to higher energy and broadened by the weakly adsorbed TMA molecules. It has been reported that weakly adsorbed noble gas atoms have similar effects on the surface state of (111) surfaces of noble metals.[17–19] Thus, the STS data suggest weak surface bonding, in agreement with the generally accepted picture that planar aromatic hydrocarbons are weakly π-bonded with the benzene rings parallel to the close-packed noble-metal substrate.[20,21]

Measurements by XPS and NEXAFS provided complementary insight into the chemical states and the bonding geometry of the TMA molecules in the structure at 300 K, corroborating the picture obtained by the STM measurements. The upper curve in Figure 3a shows the C 1s signal of the 300 K structure, and the upper curve in Figure 3b shows the O 1s signal of the 300 K structure. In the C 1s spectrum two well-separated peaks are identified, a larger one at a binding energy (BE) of 285.0 eV, which is assigned to the six carbon atoms in the benzene ring, and a smaller one at a BE of 289.1 eV, which is assigned to the three carbon atoms in the carboxyl groups, in accordance with previous reports.[10,17–22] The fit of the spectrum to Gaussian-shaped peaks with a full width at half-maximum (FWHM) of 1.4 eV is improved by adding a small additional peak with a BE of 287.3 eV, which is assigned to a small amount of carbon atoms of TMA molecules in a different chemical state or can be attributed to impurities on the surface such as adsorbed CO. The O 1s signal consists of a broad symmetric peak, which is a convolution of the signals of oxygen in hydroxyl groups (BE of 533.6 eV) and carbonyl groups (BE of 531.5 eV), in accordance with similar systems bound by hydrogen bonds between carboxyl groups.[10,18–20] The C 1s and O 1s XP spectra

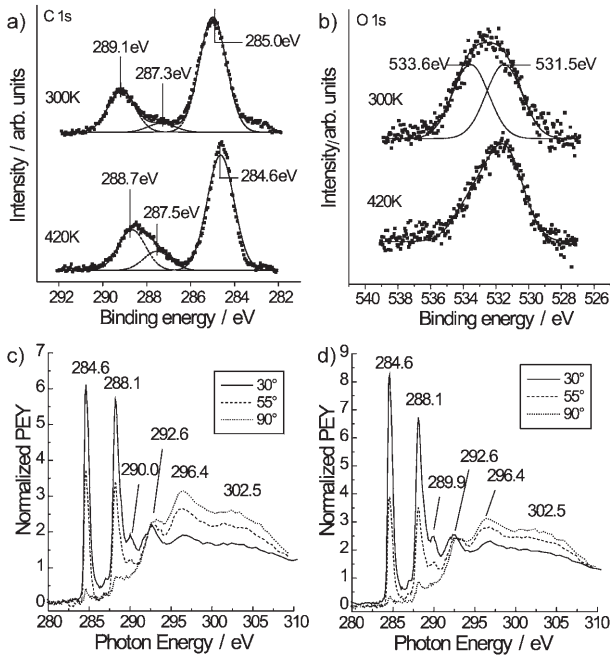

Figure 3. X-ray photoelectron spectra in a) the C 1s and b) the O 1s regions, acquired on samples annealed to 300 K (upper graphs) and 420 K (lower graphs). NEXAFS spectra of the c) 300 K and d) 420 K phasees recorded at the C K-edge. Solid and dashed lines indicate spectra obtained at different angles of incidence of the synchrotron light (90° means normal incidence to the Ag(111) surface).

clearly show that after annealing to 300 K the carboxyl groups of the TMA molecules are still protonated, and dimer hydrogen bonds are formed between carboxyl groups.

The NEXAFS spectra of the 300 K honeycomb structure are displayed in Figure 3c, in which several pronounced π^* resonances are clearly discernible. Assignment was made in analogy to that for TPA, which was thoroughly discussed in reference [22]. The π^* resonance at 284.6 eV is assigned to transitions related to the carbon atoms of the aromatic ring, whereas the prominent peak at 288.1 eV and the shoulder at 290.0 eV are assigned to transitions related to the carboxyl carbon atoms. At higher energy several σ^* transitions at 292.6, 296.4, and 302.5 eV can be identified. The π^* resonances of the benzene carbon atoms and of the carboxyl carbon atoms both show pronounced dichroism with almost completely vanishing intensity for normal photon incidence (90°). The average tilt angles calculated from the observed dichroism are $18° \pm 7°$ and $20° \pm 7°$ for the benzene and carboxyl parts of the molecule, respectively. These data indicate that the carboxyl groups are coplanar with the benzene rings. There is a significant deviation of the obtained average tilt angle from the 0° expected for perfectly flat-lying molecules. Frequently, average tilt angles of up to 10° are observed by NEXAFS spectroscopy even for perfectly flat-lying aromatic molecules on metal surfaces.[23–25] Tilting has been attributed to adsorption-induced nonplanar intramolecular distortions involving bending of the C–H bonds out of the ring plane. Therefore, a plausible explanation of our data is that the vast majority of the molecules are indeed adsorbed in a flat geometry, and the deduced average tilt angle is caused by the above-mentioned distortions and a small number of molecules deviating significantly from a flat adsorption geometry. Such molecules may be adsorbed at defects or step edges.

After annealing the sample to 420 K the open TMA honeycomb structure is transformed irreversibly into a dense-packed structure, as shown in the STM image in Figure 1b. The basic motif of this structure is a TMA quartet, a group of four closely packed TMA molecules in a rhombic arrangement with a side length of 0.9 nm and an angle of 68.4°. These quartet units are repeated in an oblique lattice with lattice constants of 1.87 ± 0.05, 1.77 ± 0.05 nm and an angle of 102°. Similar to the 300 K structure the registry of the 420 K structure with respect to the Ag(111) substrate could not be determined. The ST spectra acquired on the TMA quartet structure reveal pronounced changes in the surface electronic structure. The spectrum reproduced in Figure 2 shows a broad onset around 259.9 ± 30.9 mV with a width of 76.5 ± 23.6 mV. Again there is no spatial variation of the STS signal, hence we attribute the onset feature in the ST spectrum to the surface-state electrons. It is known that stronger adsorbate–substrate interactions can lead to substantial changes in the electronic structure of the substrate and even quenching of the surface state. The observed significant deviation of the ST spectrum of the 420 K structure from that of the weakly bound neutral adsorbate implies notable impact of the TMA quartets on the surface electronic state.[26–28]

A detailed analysis of the XPS measurements on the close-packed 420 K structure reveals a distinct change in the chemical state of the TMA molecules. The C 1s signal shown in the lower part of Figure 3a still consists of two peaks, but the smaller one at a BE of 289.0 eV is broadened relative to the small peak in the 300 K structure. The C 1s signal was fitted by three Gaussian-shaped peaks with an FWHM of 1.4 eV, and the obtained binding energies were compared to the results of the 300 K structure and to published data. The smaller peak has been deconvoluted into two peaks, one for carbon atoms in the carboxyl groups at a BE of 288.7 eV, in good agreement with the 300 K structure, and one for carbon atoms in a new state at a BE of 287.5 eV. This new peak is assigned to carbon atoms in carboxylate groups, in agreement with previous measurements.[4,8,10,35–40] Carbon atoms in the benzene ring are found at a BE of 284.6 eV, also in good agreement with the 300 K structure. The relative peak areas, with the total area of the spectrum normalized to the nine carbon atoms in a TMA molecule, were 5.9 for the benzene peak, 2.1 for the carboxyl peak, and 1.0 for the carboxylate peak. The areas of the carboxyl and carboxylate peaks sum to three carbon atoms, and this implies that the carboxylate groups have their origin in the carboxyl groups.

The O 1s signal (Figure 3b, lower curve) became asymmetric after annealing to 420 K and could no longer be fitted with two equal Gaussian-shaped peaks. Instead, the asymmetric signal clearly shows the formation of oxygen

atoms in different chemical states, in contrast to those found in the purely hydrogen-bonded honeycomb arrangement.[4,17–20] A quantitative interpretation of the O 1s signal is much more difficult than for the C 1s signal, as the chemical neighborhood and therefore the number of different kinds of oxygen atoms in the 420 K structure are not known. Therefore, we refrained from a quantitative analysis of the O 1s signal.

In summary, the appearance of new chemical states in the carbon and oxygen spectra is attributed to the often-observed deprotonation of carboxyl groups upon adsorption on metal surfaces and the formation of carboxylate groups.[5,7,9,11,29] Based on the relative peak areas in the C 1s signal, the number of carbon atoms is 2.1 in carboxyl groups and 1.0 in carboxylate groups. Considering the high symmetry of the structure, we conclude that after annealing to 420 K one out of three carboxyl groups per molecule is deprotonated and transformed into a carboxylate group.

The NEXAFS spectra of the 420 K structure are displayed in Figure 3d. Upon warming to 420 K and measuring the sample again at 300 K the dichroism of the π* resonances remains very pronounced (see Figure 3d). The calculated average tilt angles are now $14°\pm5°$ for the benzene rings and $23°\pm5°$ for the carboxyl groups. This indicates that the molecules remain in a essentially flat-lying geometry on the surface. It seems that the carboxyl groups on average are now tilted by 5–10° out of the plane of the benzene ring. Comparing the NEXAFS spectra obtained for the two phases one notices only small differences; in particular, the intensity of the carboxyl π* resonance is not much reduced relative to the π* resonance of the benzene ring. These changes are consistent with only partial deprotonation of the carboxyl groups. For complete deprotonation we would expect a much more pronounced decrease of the carboxyl π* resonance, as has been observed by us in a related system, that is, terephthalic acid (TPA) on Cu(100).[10]

Theoretical results: The deprotonation of carboxyl groups upon adsorption on metal surfaces has been observed in many other systems, but usually the oxygen atoms of the carboxylate groups bind to substrate atoms, and this tilts the whole molecule to an upright-standing configuration.[5,7,9,11,29] In contrast to these results, our STM and NEXAFS measurements for the 420 K structure clearly provide evidence for flat-lying TMA molecules containing one carboxylate group. This suggests that the carboxylate groups are engaged in lateral intermolecular binding by forming ionic hydrogen bonds with neutral carboxyl groups of the neighboring TMA molecules. A fundamental and evident precondition for the formation of ionic hydrogen bonds is that the carboxylate group is still charged and the charge is not distributed over the entire molecule or compensated by the metallic substrate. To gain information about the charge states of the partially deprotonated molecule, ab initio calculations were performed on a single TMA molecule containing one carboxylate group (denoted "deprotonated" TMA molecule in what follows). Then classical molecular dynamics calculations were performed to reproduce the quartet structure and to gain better understanding of the interplay between charged carboxylate groups and the neutral carboxyl groups.

We performed 0 K ab initio calculations of a single TMA molecule placed on a five-layer slab of Ag(111) (Figure 4). The solid curve in Figure 4a shows the response of the electronic charge density to deprotonation. This is computed from the electron densities ρ_{prot} and ρ_{deprot} of the protonated and deprotonated molecule systems as $-e\,(\rho_{deprot}-\rho_{prot})$. The atomic positions in both calculations are those obtained for the relaxed protonated molecule adsorbed on the metal surface. The electron density difference is integrated over the *xy* planes and plotted as a function of the *z* variable (the

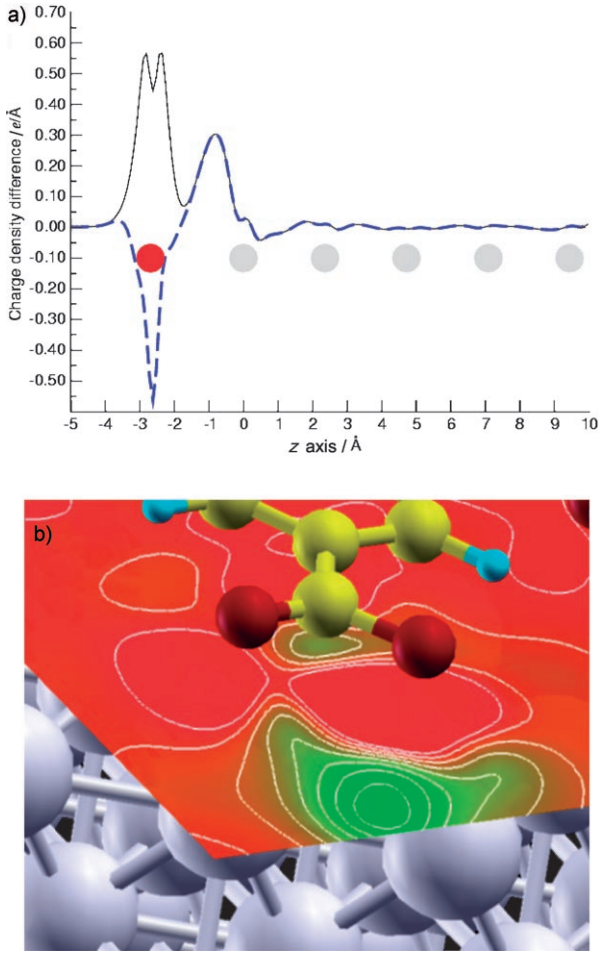

Figure 4. a) Charge-density variations upon deprotonation of a TMA molecule adsorbed on a slab of Ag(111). All quantities are integrated over the *xy* plane and plotted along the *z* direction. The blue dashed curve refers to the total charge density variation, which yields a negative surface dipole density profile. The electronic contribution to the total charge density variation is shown in the solid curve (see text). The red and gray filled circles correspond to the *z* positions of the adsorbed molecules and the first four layers of the metal substrate, respectively. b) The electron-density depletion (or positive charge-density accumulation) corresponding to the peak centered at $z=-0.9$ Å is also visible as a green lobe located under the carboxylate group (the contour plot of the density difference is taken at $z=-0.7$ Å).

origin of the z axis corresponds to the first atomic layer of the Ag surface).

Deprotonation involves loss of a proton screened by release of some electron density to the surface, so that the net final charge of the molecular ion is a value q between 0 and $-e$. The release of electron density corresponds to the prominent positive (double) peak of the solid line centered at the position $z=-2.8$ Å of the adsorbed molecule (the relaxed adsorption geometry of the molecule was in all cases flat). A second, lower peak of the solid line is centered at about -0.9 Å, that is, in the region between the molecule and the first surface layer of the metal substrate. This peak corresponds to a surface screening effect mostly localized under the missing proton (see also Figure 4b). As above, a positive peak here represents the loss upon deprotonation of some of the negative charge density originally screening the proton.

The total charge-density variation upon deprotonation is simply the sum of its electronic contribution described by the solid curve in Figure 4a and the negative contribution due to the loss of proton charge (modeled by a Gaussian of width 0.3 Å centered on the proton site and normalized to $-e$). The total charge-density variation is represented by the blue dashed line in Figure 4a, and its overall shape is that of the charge-density profile of a negative surface dipole layer. To estimate the charge q of the molecule after deprotonation we integrated the total charge density variation discussed above over the z interval "occupied" by the molecule. This interval can be taken to start at any z_0 value located well inside the vacuum region where all densities are zero and end at an upper value z_1 located between the molecular plane and the first Ag layer.

The value for z_1 was obtained by imposing the neutrality condition on the protonated molecule. The value of q was then simply obtained by integration of the blue dashed curve in Figure 4a between $z_0=-5.0$ Å and $z_1=-1.48$ Å. These calculations predict a total charge $q=-0.3e$ for the deprotonated TMA molecule. Note that in the calculations described so far and illustrated by Figure 4 the molecule/slab systems were in all cases neutral: in particular, one electron was subtracted from the overall system together with the proton to obtain the model used for the geometry in the deprotonated state. Imposing charge neutrality on the deprotonated system and repeating the calculation yields similar results, with a somewhat higher charge $q=-0.5e$ associated with the adsorbed deprotonated molecule.

Overall, these results predict the formation of a negative surface dipole layer on the Ag(111) substrate upon deprotonation, corresponding to the blue curve distribution in Figure 4a. We note that a physical picture of temperature-induced deprotonation with formation of a negative dipole lowering the electrostatic potential in the surface region is consistent with the upshift of the surface-state energy level visible in the ST spectrum of Figure 2.[26–28]

The classical MD force field can be used to model the presence of charged surface species by appropriate modification of the partial Coulomb charges. As we are investigating the possibility of supramolecular assembly between similarly charged molecular ions, the charges on the oxygen atoms of the carboxyl group after the removal of the hydrogen atom were adjusted to achieve the overall calculated total ionic charge of $q=-0.5e$ corresponding to the least favorable (most repulsive) case for assembly in our calculated range.

The partial charges used are reported in Figure 5a. As the TMA molecules are always adsorbed in a flat-lying geometry on the surface, we performed two-dimensional classical MD simulated annealing runs, with the further constraint of describing the molecules as rigid bodies. The interaction between the molecules was modeled by a superimposition of a Coulomb term obtained from the partial charges and a short-range repulsive term designed to ensure that the molecules do not overlap. The electrostatic screening of the metal surface was taken into account by introducing mirror images of the partial point charges of the potential.[30]

We then considered an isolated group of four molecules to find a stable candidate for a model structure of the quartet units revealed by the experimental observations. Consis-

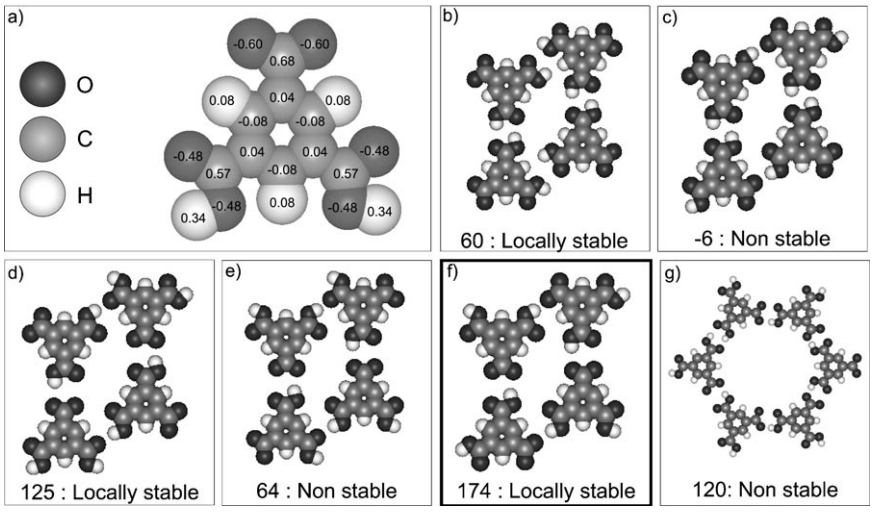

Figure 5. a) Effective atomic point charges of a deprotonated TMA molecule. The total molecular charge of $-0.5e$ (mostly localized on the carboxylate group) is consistent with the results of an ab initio calculation on a deprotonated systems of total charge -*e* (see text); b–f) Ball-and-stick models of the different investigated configurations of the quartet molecular unit are reported with indication of their stability (structures corresponding to local minima are denoted here as "metastable"). The interaction energy per molecule calculated with the classical force field is given for each structure in units of 10^{-4} a.u. g) Model of a hypothetical deprotonated honeycomb structure, which is found to be unstable in simulations using the force field.

tent with the XPS results and the high symmetry of the structure, we assumed that each molecule bore one carboxylate group. We explored the stability of different configurations by systematically changing the positions of the two remaining carboxyl protons of each TMA molecule in the unit cell. Furthermore, since the STM images showed C_2 symmetry, we limited the search to the different proton configurations that have this symmetry, as shown in Figure 5b–f. This cluster structure was used (with minor adjustments obtained by MD annealing) to produce a periodic pattern compatible with the experimental dimensions of the surface unit cell. The lowest energy structure found corresponds to the configuration shown in Figure 5f. The final equilibrium structure obtained in this way, shown in Figure 6a, is in good agreement with the experimentally observed structure. All

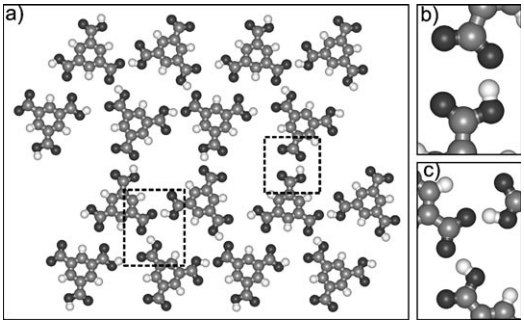

Figure 6. a) Calculated structure of the most stable configuration of the building block (Figure 5 f). The two different kinds of ionic hydrogen bonds are outlined. b) Ionic hydrogen bond between one carboxylate group and one carboxyl group. c) Ionic hydrogen bond between one carboxylate group and two carboxyl groups.

charged carboxylate groups are bound to neutral carboxyl groups, and furthermore two different kinds of carboxylate groups exist in the 420 K structure, highlighted in Figure 6a and magnified in Figure 6b and c. Figure 6b shows the first kind of ionic hydrogen bond of this structure, which stabilizes a TMA dimer in which the carboxylate group is bound to a single carboxyl group. Figure 6c shows the second kind of ionic hydrogen bond, in which the carboxylate group is bound to two carboxyl groups on different molecules. These different bonds to different molecules ultimately allow the dimers to assemble into the observed chain structure. The calculated O···O distance for both ionic hydrogen bonds was 0.256 nm.

In addition, the possibility of forming a honeycomb structure from deprotonated TMA molecules was investigated, as shown in Figure 5g. We note that a honeycomb structure undergoing a single deprotonation per molecule as shown in Figure 5g would involve the same overall number of hydrogen bonds as observed in the predicted stable structure of Figure 5f (as the overall residual number of hydrogen atoms would be the same in the two structures). However, the hexagonal arrangement would imply pairs of adjacent negatively charged and mutually repulsive oxygen atoms, located on the non-hydrogen-bonded side of facing carboxyl group pairs. This cannot happen in the denser packing experimentally observed, in which carboxyl group pairs never face each other and can thus be connected by at most one hydrogen bond. As one can see from the interaction energies reported in Figure 5, the deprotonated hexagonal phase (honeycomb structure) is significantly less stable than the densely packed structure. Thus a structural transformation would presumably occur upon deprotonation of the carboxyl groups. The preferred arrangement of the molecules upon deprotonation is determined by the concurrent need to maximize the number of hydrogen bonds, while minimizing the Coulomb repulsion between negatively charged deprotonated carboxyl groups. In this scenario, the honeycomb structure becomes unstable upon deprotonation and the system "collapses" into a more densely packed structure in which ionic hydrogen bonds play an important role. The phase transition is driven by deprotonation and is thus irreversible, consistent with the experimental findings.

In conclusion, our experiments and calculations suggest that intermolecular ionic hydrogen bonds offer novel possibilities to steer the assembly of supramolecular structures on surfaces. The realized supramolecular structures are notably stable in the absence of counterions (necessary in solvent phases to stabilize ionic hydrogen bonds) due to the charge-screening effect of the metal surface. This process implies that the energy gain resulting from intermolecular ionic hydrogen bonds exceeds that of potential molecule-to-substrate bonds. The latter depends on the chemistry of the substrates. For example, when employing Cu surfaces, deprotonated TMA or related species can be engaged in carboxylate anchoring to the surface rather than forming intermolecular ionic hydrogen bonds.[11,31] In general, chemically inert substrates like Ag and Au are more appropriate for formation of ionic hydrogen bond with adsorbed carboxylate species.

Experimental Section and Computational Methods

Measurements: All measurements were made in ultrahigh vacuum (UHV) systems equipped with standard equipment for sample cleaning and preparation. The Ag(111) surface was cleaned by repeated cycles of sputtering with 500 eV Ar^+ ions and subsequent annealing to about 800 K. Commercially available TMA (Aldrich, purity $\approx$ 95 %) was deposited onto the Ag(111) surface by means of organic molecular beam epitaxy (OMBE), with the crucible containing the TMA powder held at a temperature of 473 K during deposition. The Ag(111) substrate was kept at a temperature of about 100 K during deposition, followed by annealing steps to 300 and 420 K. The annealing time had no influence on the self-ordering process. Annealing in the temperature range between 300 and 420 K led to mixtures of the two phases. The coverage was always in the submonolayer range; typically one-quarter to one-third of the Ag(111) surface was covered by TMA molecules. STM and STS data were acquired using a home-built Besocke type STM operated at a temperature of 5 K. The STM measurements were performed in the constant-current mode with electrochemically etched W tips. ST spectra were recorded using a lock-in amplifier set to a frequency of 5 kHz and a modulation amplitude of 10 mV. The cleanness of the tip was checked by acquiring ST spectra on the clean Ag (111) surface, which showed the typical step-

like feature of the two-dimensional surface state.[32–34] The XPS and NEXAFS data were acquired at the HE-SGM Beamline of the BESSY II Synchrotron Radiation Facility in Berlin at a temperature of 300 K. The XP spectra were recorded with beam energies of 400 eV for the carbon 1s peak and 670 eV for the oxygen 1s peak, both with a pass energy of the analyzer offset to 50 eV. Additional spectra were taken with the $Al_{K\alpha}$ radiation of a laboratory source and a pass energy of the analyzer of 100 eV. The spectra were referenced to the Ag $3d_{5/2}$ line at 368.2 eV. The XP spectra were fitted after linear background subtraction with a suitable number of Gaussian-shaped peaks, linked to carbon and oxygen atoms in different states within the structures. These peaks were allocated to the different states of carbon and oxygen in the TMA molecules, and the areas of the peaks were used as a measure for the number of atoms in these states.[10,15–40] All NEXAFS spectra were recorded in the partial electron yield mode (retarding voltage −150 eV) with a double-channel plate as electron detector. For the methods used for energy calibration and normalization of the spectra, see reference [10].

Calculations: In our theoretical investigation we used a combination of classical and ab initio molecular dynamics (MD) methods. All first-principles calculations were carried out by using the Car–Parrinello method,[41] with Troullier Martins norm-conserving pseudopotentials and a gradient-corrected exchange-correlation functional.[42,43] The metal systems were treated within the scheme of reference [44] with a smearing energy width of $E_s = 0.25$ eV. Sampling of the Brillouin zone was limited to the gamma point only. The plane-wave expansion was truncated at an energy cutoff of 50 Ry. In calculations including surfaces this cutoff was increased to 80 Ry. We initially performed ab initio simulations of isolated molecules. The electron densities were used to determine a classical potential according to the established procedure detailed references [45–47] The Poisson equation was first solved to obtain the electrostatic potential. The effective partial Coulomb point charges, positioned on the core ions, were then determined from the best fit of the electrostatic potential outside a van der Waals exclusion area defined by the atomic effective radii (0.38, 0.33, and 0.29 nm for C, O, and H atoms respectively).[45]

Acknowledgements

This research was funded by the program EUROCORES-SONS of the European Science Foundation. A.C. acknowledges funding from Area Science Park of Trieste.

[1] J. V. Barth, G. Constantini, K. Kern, *Nature* **2005**, *437*, 671–679.
[2] J. V. Barth, J. Weckesser, N. Lin, A. Dmitriev, K. Kern, *Appl. Phys. A* **2003**, *76*, 645–652.
[3] S. De Feyter, F. C. De Schryver, *Chem. Soc. Rev.* **2003**, *32*, 139–150.
[4] B. Immaraporn, P. Ye, A. J. Gellman, *J. Phys. Chem. B* **2004**, *108*, 3504–3511.
[5] N. Lin, D. Payer, A. Dmitriev, T. Strunskus, C. Wöll, J. V. Barth, K. Kern, *Angew. Chem.* **2005**, *117*, 1512–1515; *Angew. Chem. Int. Ed.* **2005**, *44*, 1488–1491.
[6] M. Bowker, E. Rowbotham, F. M. Leibsle, S. Haq, *Surf. Sci.* **1996**, *349*, 97–110.
[7] J. G. Lee, J. Ahner, D. Mocuta, S. Denev, J. T. Yates, *J. Chem. Phys.* **2000**, *112*, 3351–3357.
[8] B. Parker, B. Immaraporn, A. J. Gellmann, *Langmuir* **2001**, *17*, 6638–6646.
[9] D. S. Martin, R. J. Cole, S. Haq, *Surf. Sci.* **2003**, *539*, 171–181.
[10] S. Stepanow, T. Strunskus, M. Lingenfelder, A. Dmitriev, H. Spillmann, N. Lin, J. V. Barth, C. Wöll, K. Kern, *J. Phys. Chem. B* **2004** *108*, 19392–19397.
[11] A. Dmitriev, N. Lin, J. Weckesser, J. V. Barth, K. Kern, *J. Phys. Chem. B* **2002**, *106*, 6907–6912.
[12] M. Meot-Ner (Mautner), *Chem. Rev.* **2005**, *105*, 213–284.
[13] D. Braga, A. Angelino, E. Tagliavini, F. Grepioni, *J. Chem. Soc. Dalton Trans.* **1998**, 1961–1968.
[14] S. Griessl, M. Lackinger, M. Edelwirth, M. Hietschold, W. M. Heckl, *Single Mol.* **2002**, *3*, 25–31.
[15] Y. Ishikawa, A. Ohira, M. Sakata, C. Hirayama, M. Kunitake, *Chem. Commun.* **2002**, *22*, 2652–2653.
[16] G. J. Su, H. M. Zhang, L. J. Wan, C. L. Bai, T. Wandlowski, *J. Phys. Chem. B* **2004**, *108*, 1931–1937.
[17] R. Paniago, R. Matzdorf, G. Meister, A. Goldmann, *Surf. Sci.* **1995**, *325*, 336–342.
[18] H. Hövel, B. Grimm, B. Reihl, *Surf. Sci.* **2001**, *477*, 43–49.
[19] T. Andreev, I. Barke, H. Hövel, *Phys. Rev. B* **2004**, *70*, 2054261–20542613.
[20] S. Lehwald, H. Ibach, J. E. Demuth, *Surf. Sci.* **1978**, *78*, 577–590.
[21] P. Yannoulis, R. Dudde, K. H. Frank, E. E. Koch, *Surf. Sci.* **1987**, *189*, 519–528.
[22] T. Okajima, K. Teramoto, R. Mitsumoto, H. Oji, Y. Yamamoto, I. Mori, H. Ishii, Y. Ouchi, K. Seki, *J. Phys. Chem. A* **1998**, *102*, 7093–7099.
[23] C. Mainka, P. S. Bagus, A. Schertel, T. Strunskus, M. Grunze, C. Wöll, *Surf. Sci.* **1995**, *341*, L1055 L1060.
[24] K. Weiss, S. Gebert, M. Wühn, H. Wadepohl, C. Wöll, *J. Vac. Sci. Technol. A* **1998**, *16*, 1017–1022.
[25] S. Lukas, S. Söhnchen, G. Witte, C. Wöll, *ChemPhysChem* **2004**, *5*, 266–270.
[26] R. Paniago, R. Matzdorf, G. Meister, A. Goldmann, *Surf. Sci.* **1995**, *325*, 336–342.
[27] W. Jacob, V. Dose, A. Goldmann, *Appl. Phys. A* **1986**, *41*, 145–150.
[28] S. A. Lindgren, J. Paul, L. Wallden, *Surf. Sci.* **1982**, *117*, 426–433.
[29] B. G. Frederick, Q. Chen, F. M. Leibsle, M. B. Lee, K. J. Kitching, N. V. Richardson, *Surf. Sci.* **1997**, *394*, 1–25.
[30] M. Vladimirova, M. Stengel, A. De Vita, A. Baldereschi, M. Böhringer, K. Morgenstern, R. Berndt, W. D. Schneider, *Europhys. Lett.* **2001**, *56*, 254–260.
[31] A. Dmitriev, H. Spillmann, S. Stepanow, Th. Strunskus, Ch. Wöll, A. P. Seitsonen, M. Lingenfelder, N. Lin, J. V. Barth, K. Kern, *ChemPhysChem* **2006**, *7*, 2197–2204.
[32] J. Li, W. D. Schneider, R. Berndt, O. R. Bryant, S. Crampin, *Phys. Rev. Lett.* **1998**, *81*, 4464–4467.
[33] L. Bürgi, L. Petersen, H. Brune, K. Kern, *Surf. Sci.* **2000**, *447*, L157–L161.
[34] L. Bürgi, N. Knorr, H. Brune, M. A. Schneider, K. Kern, *Appl. Phys. A* **2002**, *75*, 141–145.
[35] L. H. Dubois, B. R. Zegarski, R. G. Nuzzo, *Langmuir* **1986**, *2*, 412–417.
[36] S. W. Han, S. W. Joo, T. H. Ha, Y. Kim, K. Kim, *J. Phys. Chem. B* **2000**, *104*, 11987–11995.
[37] M. Wühn, J. Weckesser, C. Wöll, *Langmuir* **2001**, *17*, 7605–7612.
[38] G. Axelson, U. Ericson, A. Fahlman, K. Hamrin, J. Hedman, R. Nordberg, R. Nordling, K. Siegbahn, *Nature* **1967**, *213*, 70–71.
[39] D. L. Hoof, D. G. Tisley, R. A. Walton, *J. Chem. Soc. Dalton Trans.* **1973**, *2*, 200–204.
[40] U. Gelius, P. F. Hedén, J. Hedman, B. J. Lindberg, R. Manne, R. Nordberg, C. Nordling, K. Siegbahn, *Phys. Scr.* **1970**, *2*, 70–80.
[41] R. Car, M. Parrinello, *Phys. Rev. Lett.* **1985**, *55*, 2471–2474.
[42] N. Troullier, J. L. Martins, *Phys. Rev. B* **1991**, *43*, 1993–2006.
[43] J. P. Perdew, Y. Wang, *Phys. Rev. B* **1992**, *45*, 13244–13249.
[44] J. VandeVondele, A. De Vita, *Phys. Rev. B* **1999**, *60*, 13241–13244.
[45] M. Vladimirova, G. Trimarchi, A. Baldereschi, J. Weckesser, K. Kern, J. V. Barth, A. De Vita, *Acta Mater.* **2004**, *52*, 1589–1595.
[46] M. Böhringer, K. Morgenstern, W. D. Schneider, R. Berndt, F. Mauri, A. De Vita, R. Car, *Phys. Rev. Lett.* **1999**, *83*, 324–327.
[47] J. V. Barth, J. Weckesser, G. Trimarchi, M. Vladimirova, A. De Vita, C. Cai, H. Brune, P. Günter, K. Kern, *J. Am. Chem. Soc.* **2002**, *124*, 7991–8000; J. Weckesser, A. De Vita, J. V. Barth, C. Cai, K. Kern, *Phys. Rev. Lett.* **2001**, *87*, 096101.

Received: September 14, 2006
Revised: November 16, 2006
Published online: February 9, 2007

